Feedback and $\mathcal{PT}$ Symmetry in a class of Active LCR Circuits

Miguel Mayosky, , Alejandro Veiga ,
Carlos García Canal and Huner Fanchiotti.

April 21, 2023

Abstract

Systems with non-Hermitian Hamiltonians, especially those exhibiting parity-time ($\mathcal{PT}$) symmetry, are of particular interest as they can describe physical open systems with balanced loss into and gain from the environment. In this context, the study of eigenvalue locations and the corresponding phase transitions as a function of the degree of non-Hermiticity γ is accomplished hereby using feedback theory. This approach provides insight about the behavior of these systems and allows generalization of the results for higher-order ones. The proposed ideas are analyzed in detail for a class of coupled resonant circuit chains.

1 Introduction

The basic property of the operators that represent observables in Quantum Mechanics is Hermiticity, since a Hermitian operator has real eigenvalues, which are the measurable quantities related to a physical magnitude. Consequently, Hermiticity of the Hamiltonian $\mathcal{H}$, the operator representing the energy of the system, is a fundamental postulate in quantum mechanics. However, open systems exhibiting flows of energy, particles, and information, are usually described by non-Hermitian Hamiltonians, in general associated with the decay of the norm of a quantum state. Among the non-Hermitian Hamiltonians, those that exhibit parity-time ($\mathcal{PT}$) symmetry are of particular interest because they can

Miguel Mayosky is with LEICI, Departamento de Electrotecnia, Facultad de Ingeniería, Universidad Nacional de La Plata (UNLP), La Plata, Argentina, and Comisión de Investigaciones Científicas de la Provincia de BuenosAires (CICpBA), Argentina. (e-mail: mayosky@ing.unlp.edu.ar)

Alejandro Veiga is with LEICI, Departamento de Electrotecnia, Facultad de Ingeniería, Universidad Nacional de La Plata (UNLP), La Plata, Argentina and Consejo Nacional de Investigaciones Científicas y Técnicas (CONICET). (e-mail: alejandro.veiga@ing.unlp.edu.ar

Carlos García Canal and Huner Fanchiotti are with IFLP/CONICET and Departamento de Física, Universidad Nacional de La Plata (UNLP), C.C.67, 1900, La Plata, Argentina. (e-mail:cgarciacanal@fisica.unlp.edu.ar, huner@fisica.unlp.edu.ar)

admit real eigenvalues while describing physical open systems with balanced loss into and gain from the surrounding environment [1]. Those $\mathcal{PT}$ systems may have a real energy spectrum, although in general are non-Hermitian. Besides, as some parameter γ (associated with the degree of non-Hermiticity of $\mathcal{H}$) changes, a spontaneous $\mathcal{PT}$ symmetry breaking occurs and eigenvalues become complex [2]. For a more detailed explanation see Appendix A

The non-Hermitian description can be applied also to many non-conservative classical systems, providing a true analogy to explore unconventional wave phenomena in many other fields. In particular, electronic circuits consisting of identical resonators with linear couplings represent an interesting platform to evaluate all the phenomena encountered in systems with generalized $\mathcal{PT}$ symmetries, such as biological oligomers [3]. Many of such devices, that allow direct observation of a "phase transition" from a real to a complex eigenfrequency spectrum are reported in the literature [4], [6], [7]. For these systems, feedback turns out to play a relevant role in symmetry breaking.

In this paper, eigenvalues behavior and their corresponding phase transitions as a function of the degree of non-Hermiticity γ is analyzed using automatic control tools, particularly the root-locus technique [8]. To this end, the state matrix of the system is interpreted in the context of a linear feedback loop, with γ as a variable gain. Then, the characteristic equation is rewritten in the root-locus form [9], which allows the drawing of the "closed loop" pole paths (that is, the roots of the characteristic equation) as continuous trajectories in the Laplace complex plane. The resulting plot provides insight into the behavior of the system, and opens the door to the analysis and synthesis of more complex ones, in particular chains of identical oscillators, which can be applied, for instance, to the design of high gain sensors [10], [11], [12].

The proposal is first applied to an electronic circuit consisting of two LC oscillators coupled by a gyrator [3], [4], [13], [14], and symmetric negative and positive resistors [15], [16]. The use of a gyrator simplifies the analysis, and avoids the need for magnetic (mutual inductance) couplings, allowing prototypes to be constructed from standard devices [17]. Spice simulations are presented, showing their feasibility. Besides, the analysis can be extended to systems of arbitrary order.

The text is organized as follows: Section 2 presents the electronic circuit proposed as a typical example of a non-Hermitian system. Section 3 analyzes such systems as a class of linear feedback loops, with γ being a variable gain. In section 4 the trajectories described by the eigenvalues as a function of γ are analyzed using the root-locus technique, followed by simulation results in section 5. Section 6 extends the results to oligomers of order n. Section 7 resumes the conclusions and suggests further lines.

2 A non-Hermitian electronic circuit

A typical circuit exhibiting $\mathcal{PT}$ symmetry is depicted in Fig. 1. It consists of two identical LC pairs, connected through a gyrator of transconductance G_g.

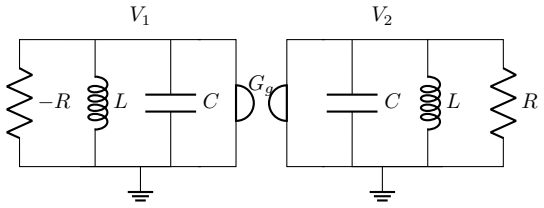

Figure 1: Non-Hermitian circuit using a Gyrator

One of the circuits has a negative resistance $-R$, which provides the energy income, and the other has a positive resistance of identical value R, accounting for energy losses. Similar topologies have been used for modeling $\mathcal{PT}$ systems in the literature [3], [4], [13]. Circuit equations are straightforward:

$$\begin{cases} \ddot{V}_1 + V_1 \frac{1}{LC} - \dot{V}_1 \frac{1}{RC} + \dot{V}_2 \frac{G_g}{C} = 0 \\ \ddot{V}_2 + V_2 \frac{1}{LC} + \dot{V}_2 \frac{1}{RC} - \dot{V}_1 \frac{G_g}{C} = 0 \end{cases} \tag{1}$$

The $\mathcal{PT}$ symmetry becomes evident, as interchanging subindex 1 by 2 and time t by $-t$ in the above equations keep them invariant [3]. As usual in circuit analysis, these two second-order equations can be written as a system of four first-order equations using, for instance, the change of variables $[x_1 \;\; x_2 \;\; x_3 \;\; x_4]^T = [V_1 \;\; V_2 \;\; \dot{V}_1 \;\; \dot{V}_2]^T$, or any linear combination of those. Then, the state equation $\dot{x} = Ax$ becomes:

$$\begin{bmatrix} \dot{x}_1 \\ \dot{x}_2 \\ \dot{x}_3 \\ \dot{x}_4 \end{bmatrix} = \begin{bmatrix} 0 & 0 & 1 & 0 \\ 0 & 0 & 0 & 1 \\ -\frac{1}{LC} & 0 & \frac{1}{RC} & -\frac{G_g}{C} \\ 0 & -\frac{1}{LC} & \frac{G_g}{C} & -\frac{1}{RC} \end{bmatrix} \begin{bmatrix} x_1 \\ x_2 \\ x_3 \\ x_4 \end{bmatrix} \tag{2}$$

Let us call

$$\omega_0^2 = \frac{1}{LC} \;\; ; \;\; \gamma = \frac{1}{RC} \;\; ; \;\; \gamma_g = \frac{G_g}{C}$$

Here γ accounts for the degree of non-Hermiticity. The state matrix A reads

$$A = \begin{bmatrix} 0 & 0 & 1 & 0 \\ 0 & 0 & 0 & 1 \\ -\omega_0^2 & 0 & \gamma & -\gamma_g \\ 0 & -\omega_0^2 & \gamma_g & -\gamma \end{bmatrix} \tag{3}$$

Equivalence to a quantum system can be written from eq.(2) using a Liouvillian formalism [3], [5] as

$$\frac{d\Psi}{d\tau} = \mathcal{L}\Psi \tag{4}$$

with $\mathcal{L} = A$, $\Psi = x$, and effective Hamiltonian $H_{\text{eff}} = i\mathcal{L}$. Thus, the eigenvalues of H_{eff} can be studied directly from those of A (real eigenvalues of H_{eff} correspond to pure imaginary eigenvalues of A). The characteristic equation for A results

$$F(s) = s^4 + s^2(\gamma_g^2 - \gamma^2 + 2\omega_0^2) + \omega_0^4 = 0, \tag{5}$$

which being a bi-quadratic equation has roots:

$$\begin{aligned} \lambda_{1,2} = &\quad \pm\sqrt{\frac{-(\gamma_g^2 - \gamma^2 + 2\omega_0^2) + \sqrt{(\gamma_g^2 - \gamma^2 + 2\omega_0^2)^2 - 4\omega_0^4}}{2}} \\ \lambda_{3,4} = &\quad \pm\sqrt{\frac{-(\gamma_g^2 - \gamma^2 + 2\omega_0^2) - \sqrt{(\gamma_g^2 - \gamma^2 + 2\omega_0^2)^2 - 4\omega_0^4}}{2}} \end{aligned} \tag{6}$$

The location of these roots is analyzed in detail in the following sections.

3 The Non-Hermitian circuit as a feedback system

It is interesting to analyze the behavior of the eigenvalues of the system as the parameter γ changes. To this end, the system can be studied in the context of feedback theory, as a "pure" Hermitian system

$$A_h = \begin{bmatrix} 0 & 0 & 1 & 0 \\ 0 & 0 & 0 & 1 \\ -\omega_0^2 & 0 & 0 & -\gamma_g \\ 0 & -\omega_0^2 & \gamma_g & 0 \end{bmatrix}, \tag{7}$$

with the linear state feedback

$$A_f = \begin{bmatrix} 0 & 0 & 0 & 0 \\ 0 & 0 & 0 & 0 \\ 0 & 0 & \gamma & 0 \\ 0 & 0 & 0 & -\gamma \end{bmatrix}, \tag{8}$$

Matrix A_f contains the parameter γ accounting for the degree of non-Hermiticity, as depicted in Fig. 2. The range of γ values that ensure that all closed loop poles (eigenvalues of A) remain in the imaginary axis corresponds to a non-Hermitic Hamiltonian with real eigenvalues. In this way, the $\mathcal{PT}$ behavior of the system is directly related to its closed-loop stability as γ varies.

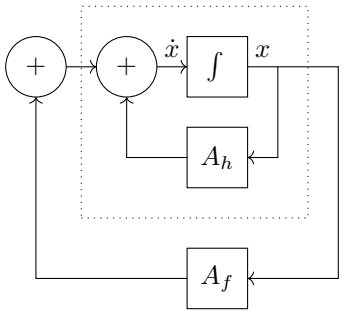

Figure 2: Non-Hermitian system. The dotted box represents the Hermitian system, with A_f as a linear state feedback.

3.1 Rewriting the characteristic equation

The location of the eigenvalues of matrix A as a function of a parameter can be analyzed using the root-locus technique [8], [9], [18]. To this end, the characteristic equation $F(s)$ is rewritten in the so-called root-locus form:

$$F(s) = 1 + KG(s) = 0 \tag{9}$$

with K being a variable gain and $G(s)$ a fixed rational function of the Laplace variable s. The root-locus is simply the plot of all points in the complex plane $s = \sigma + i\omega$ which verify $\|KG(s)\| = 1$ and $\angle(KG(s)) = 2(n+1)\pi$, that is, the roots of the characteristic equation for each value of the parameter K. The methodology provides a set of simple rules to plot the diagram without the need for solving the characteristic equation roots, and gives insight into the behavior of the system as the parameter γ changes. Operating on eq.(5) gives:

$$s^4 + s^2(\gamma_g^2 + 2\omega_0^2) + \omega_0^4 - s^2\gamma^2 = 0 \tag{10}$$

$$1 - \gamma^2 \frac{s^2}{s^4 + s^2(\gamma_g^2 + 2\omega_0^2) + \omega_0^4} = 0 \tag{11}$$

which resembles eq.(9), with

$$G(s) = \frac{s^2}{s^4 + s^2(\gamma_g^2 + 2\omega_0^2) + \omega_0^4} \tag{12}$$

and $K = -\gamma^2$. The root-locus diagram can be done manually, applying the standard rules of construction (as customary among control practitioners), or using any control analysis software. The diagram starts on the open-loop poles (the eigenvalues of the Hermitian system), and ends on the zeros of $G(s)$ for $\gamma \to \infty$.

4 Root-locus and the path to exceptional points

The starting point for the diagram is for the $\gamma = 0$ condition, that is, the Hermitian case. The eigenvalues for this condition are

$$\begin{aligned} \lambda^h_{1,2} = &\quad \pm\frac{1}{\sqrt{2}}\sqrt{-(\gamma_g^2 + 2\omega_0^2) + \sqrt{(\gamma_g^2 + 2\omega_0^2)^2 - 4\omega_0^4}} \\ \lambda^h_{3,4} = &\quad \pm\frac{1}{\sqrt{2}}\sqrt{-(\gamma_g^2 + 2\omega_0^2) - \sqrt{(\gamma_g^2 + 2\omega_0^2)^2 - 4\omega_0^4}} \end{aligned} \tag{13}$$

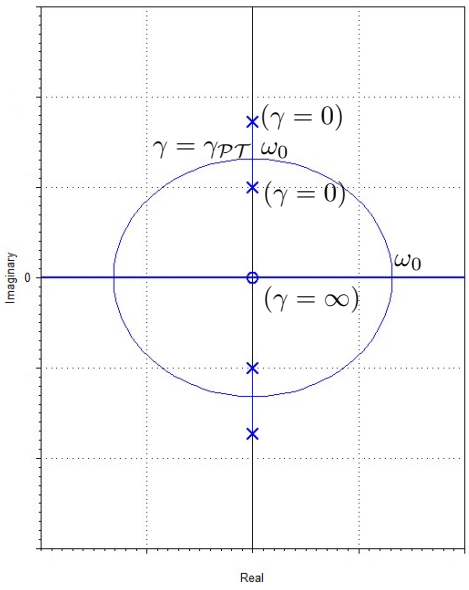

Figure 3: Root-locus of the non-Hermitian circuit. The diagram shows real vs. imaginary parts of the eigenvalues of matrix A as the parameter $-\gamma^2$ varies from 0 to ∞.

These values are pure imaginary, given that $(\gamma_g^2 + 2\omega_0^2)^2 > 4\omega_0^4$ and $(\gamma_g^2 + 2\omega_0^2) > \sqrt{(\gamma_g^2 + 2\omega_0^2)^2 - 4\omega_0^4}$. This corresponds to a pair of separate peaks in the frequency response. As γ^2 increases, the roots move on the imaginary axis, getting closer until they coincide for $\gamma = \gamma_{\mathcal{PT}}$ at $\omega = \omega_0$. In such a case a multiple pole on the imaginary axis appears. This means that the characteristic equation and its derivative must vanish. Thus, the condition to find $\gamma_{\mathcal{PT}}$ is $\frac{\partial G(s)}{\partial s} = 0$. From this analysis results:

$$\gamma_{\mathcal{PT}} = \gamma_g \tag{14}$$

which in turn involves

$$R = \frac{1}{G_g} \tag{15}$$

Interestingly enough, this condition corresponds to an "adapted" circuit, that is, one in which the Maximum Power Transfer Theorem is verified [19] [20]. The overall shape of the root-locus diagram is shown in Fig. 3. For $\gamma > \gamma_{\mathcal{PT}}$, eigenvalues become complex, and describe a circle of radius ω_0. In this condition, the two oscillation modes have the same frequency, associated with exponential envelopes of the same value but different signs (one stable and the other unstable). In the frequency response this corresponds to a single peak with decreasing quality factor Q [21] as γ grows, due to the increment in the real part of the poles (dissipation). The presence of an unstable mode precludes measurements on the experimental circuit, but the results are still clearly visible in Spice simulations. For $\gamma \to \infty$ the plot has an asymptotic behavior, with two roots going to ∞ and two approaching the pair of zeros at $s = 0$.

5 Methods

5.1 Spice model

The proposed circuit can be simulated using standard packages such as LT-Spice [22]. Although a gyrator is not included in the standard LT-Spice libraries, it can be easily implemented using two voltage-dependent current sources [13]. Initial conditions for the simulation are set by the initial capacitor voltages and inductor currents. For this example, circuit values were chosen as $L = 1mHy$, $C = 0.1\mu F$, $G_g = 1mS$, resulting in $\omega_0 = 100Kr/s$ and $\gamma_g = 10Kr/s$, for an oscillation frequency $f_0 = \frac{\omega_0}{2\pi} \cong 16kHz$. The root-locus is shown inf Fig. 4. Open loop ($\gamma = 0$) poles are located at $\pm 95,12492e{+}003i$ and $\pm 105,1249e{+}003i$, respectively.

5.2 Symmetry breaking and exceptional points.

Figure 4 shows the results of the simulations. The root-locus is presented in Figure 4(a), for $0 \leq \gamma < \infty$. The small box indicates the zone where the $\mathcal{PT}$ symmetry is broken. There are another two break points at $s = \pm\omega_0$, where the eigenvalues of A become real. In Figure 4(b) the normalized imaginary and real parts of the "closed loop" system are displayed versus the normalized degree of Hermiticity, for values of γ around the symmetry break condition. In Figure 5 the time response is displayed for different pole locations, after and before the ($\mathcal{PT}$) symmetry breaking occurs. Initial conditions for eq. 1 are set as an initial charge in the "left" capacitor. For each case, the inset shows the corresponding fft. In the non-Hermitian range of operation, there are two well-defined peaks, that come closer as γ approaches $\gamma_{\mathcal{PT}}$. Once the symmetry is broken, there is a single peak in the frequency response, which gets wider (decreasing quality factor Q) as the real parts of the roots increase. The root-locus provides a

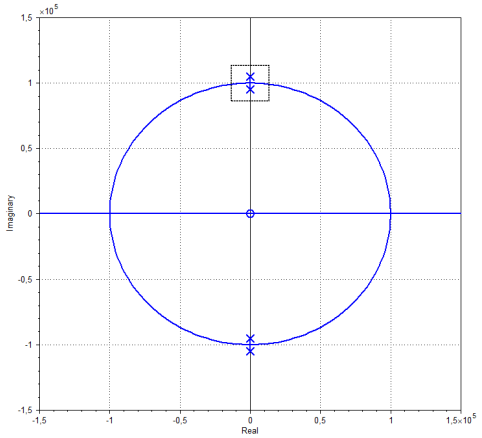

(a)

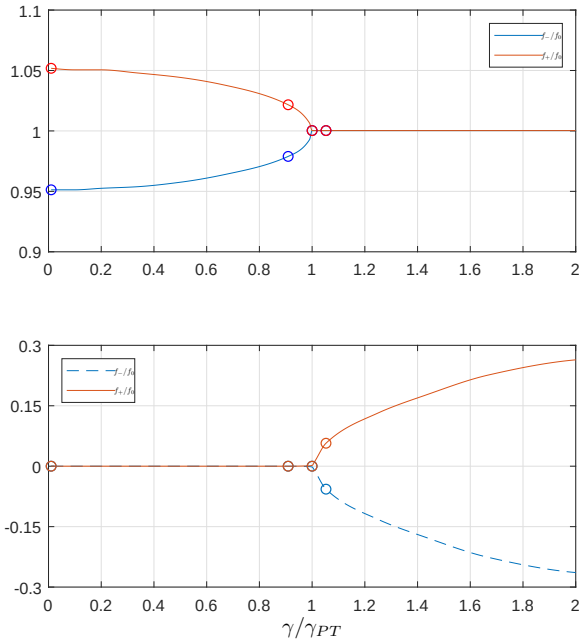

(b)

Figure 4: Simulation results. (a) Root-locus of the closed loop eigenvalues of matrix A in the Laplace plane s. Box indicates the region where Hermiticity breaks. The complete plot shows two exceptional points corresponding to $\gamma = \gamma_g$, where Hermiticity is spontaneously lost, and two additional breakpoints when the eigenvalues become purely real. (b) Normalized imaginary and real components of the eigenvalues vs. normalized degree of Hermiticity, for values of R around the exceptional point (Box)

.

simple way to interpret these results as a single graph. The phase difference between V_1 and V_2 can be appreciated in the slow envelopes in Figure 4. It varies from $\pi/2$ for the $\gamma = 0$ condition in Figure 4(a) to 0 in the exceptional point, Figure 4(c).

The overall shape of the diagram is preserved even if the coupling between oscillators is changed to any linear mechanism, for instance, a physical inductor or the mutual inductance coupling between inductors [6], the only difference being in the relative phase of the fast oscillations. In the gyrator case, such oscillations are in phase. This can be seen in Figure 5.

6 Generalization

The above results can be generalized to a chain of n coupled oscillators, using the same tools. The $2n \times 2n$ state matrix has four $n \times n$ blocks with the general form

$$A = \left[\begin{array}{c|c} A_{11} & A_{12} \\ \hline A_{21} & A_{22} \end{array}\right] = \left[\begin{array}{c|ccccc} 0 & \multicolumn{5}{c}{I_n} \\ \hline & \gamma & -\gamma_g & \dots & 0 & 0 \\ & \gamma_g & 0 & -\gamma_g & 0 & 0 \\ (-\omega_0^2) \times I_n & 0 & \ddots & \ddots & \ddots & \vdots \\ & \vdots & 0 & \gamma_g & 0 & -\gamma_g \\ & 0 & \dots & 0 & \gamma_g & -\gamma \end{array}\right] \tag{16}$$

with I_n a $n \times n$ identity matrix. The lower right block is a tridiagonal matrix (Toeplitz in the Hermitian case), which simplifies determinant calculation [23], [24]. This structure has important consequences for the root-locus:

> The relative degree of $G(s)$ (that is, the difference between the number of finite poles and zeros) is always $m = 2$, because s^n does not have γ as a coefficient, as s^{n-2} does.
>
> The independent term of the characteristic equation is ω_0^n (also independent of γ), which means that in the numerator or $G(s)$ there is always a double zero at the origin of the s plane.

Therefore, the root-locus diagram for all oligomers described by A will have only two asymptotes (that is, the behavior of the diagram as $s \to \infty$), which imply that only two eigenvalues remain complex as $\gamma \to \infty$, as in the dimer case. This is not surprising, because only the first and last oscillators have gain

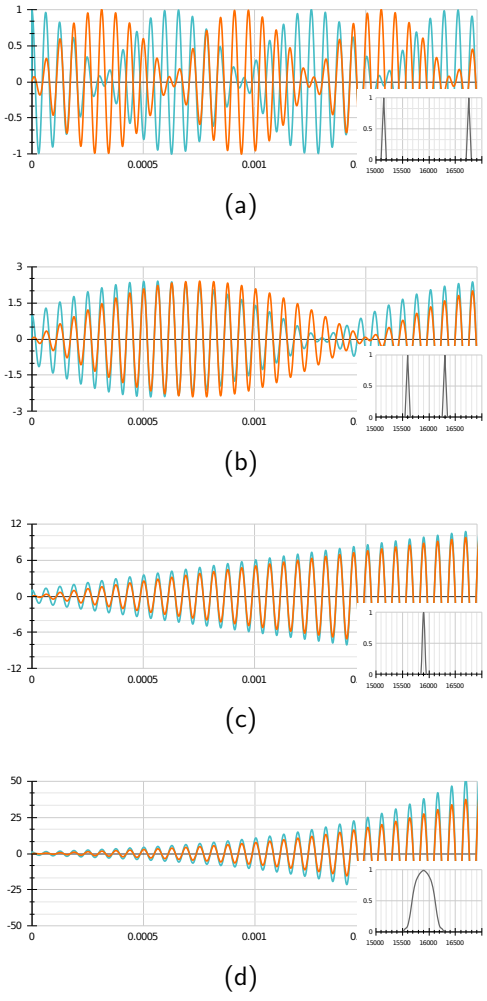

Figure 5: Simulation results. Time response: (a) Hermitic circuit. (b) Non-Hermitic circuit response for $\gamma < \gamma_{\mathcal{PT}}$. (c) and (d): Response for $\gamma > \gamma_{\mathcal{PT}}$, showing the widening of the spectra as the real part of the eigenvalues rises. The insets show the corresponding fft. Both V_1 and V_2 present a fast oscillation $(\lambda_1 + \lambda_3)$ with a slow envelope $(\lambda_1 - \lambda_3)$. Gyrator coupling ensures that the fast oscillations are always in phase, while the phase between the slow envelopes varies from $\pi/2$ to 0 as the parameter γ ranges from 0 (Hermitian) to $\gamma_{\mathcal{PT}}$ (symmetry break).

and losses, respectively. Being a block matrix, the eigenvalues in eq. 16 can be calculated as [23]:

$$det(SI - A) = det(s(sI_n - A_{22}) + \omega_0^2 I_n) = det(B) \tag{17}$$

with I_n a $n \times n$ identity matrix. Therefore, B is a $n \times n$ tridiagonal matrix with the following regular structure:

$$B = \begin{bmatrix} s(s-\gamma)+\omega_0^2 & s\gamma_g & \dots & 0 & 0 \\ -s\gamma_g & (s^2+\omega_0^2) & s\gamma_g & 0 & 0 \\ 0 & \ddots & \ddots & \ddots & \vdots \\ \vdots & 0 & -s\gamma_g & (s^2+\omega_0^2) & s\gamma_g \\ 0 & \dots & 0 & -s\gamma_g & s(s+\gamma)+\omega_0^2 \end{bmatrix} \tag{18}$$

which can be written as

$$B = \begin{bmatrix} b_n & s\gamma_g & \dots & 0 & 0 \\ -s\gamma_g & b_{n-1} & s\gamma_g & 0 & 0 \\ 0 & \ddots & \ddots & \ddots & \vdots \\ \vdots & 0 & -s\gamma_g & b_2 & s\gamma_g \\ 0 & \dots & 0 & -s\gamma_g & b_1 \end{bmatrix} \tag{19}$$

The determinant d of matrix B can be easily calculated for any dimension n using the following recursion:

$$\begin{aligned} d_0 &= 1 && (20)\\ d_1 &= b_1 && (21)\\ d_2 &= b_2 d_1 + s^2\gamma_g^2 d_0 && (22)\\ &\vdots \\ d_i &= b_i d_{i-1} + s^2\gamma_g^2 d_{i-2} && (23) \end{aligned}$$

An interesting example is the trimer, depicted in Fig. 6. The characteristic equation is

$$F(s) = s^6 + s^4(3\omega_0^2 + 2\gamma_g^2 - \gamma^2) + s^2(3\omega_0^4 + 2\gamma_g^2\omega_0^2 - \gamma^2\omega_0^2) + \omega_0^6 \tag{24}$$

Following the procedure just described, we have

$$\begin{aligned} G(s) =& \frac{s^2(s^2+\omega_0^2)}{s^6 + s^4(3\omega_0^2 + 2\gamma_g^2) + s^2(3\omega_0^4 + 2\gamma_g^2\omega_0^2) + \omega_0^6} = \\ =& \frac{s^2(s^2+\omega_0^2)}{(s^4 + 2s^2(\omega_0^2+\gamma_g^2) + \omega_0^4)(s^2+\omega_0^2)} \end{aligned} \tag{25}$$

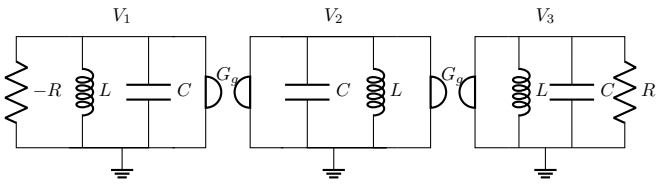

Figure 6: Non-Hermitian trimer using Gyrators

and $K = -\gamma^2$. The term $(s^2 + \omega_0^2)$ is a factor of both numerator and denominator, which implies a superposition of a pole and a zero in $G(s)$. In fact, all odd-order oligomers have an open-loop pole at ω_0. As the diagram starts in the poles of $G(s)$ and ends in its zeros [9], this implies that the pole in $\omega = \omega_0$ remains fixed. The other two poles approach each other, and coincide, also in $\omega = \omega_0$ for $\gamma = \gamma_{\mathcal{PT}} = \sqrt{2}\gamma_g$. The resulting root-locus diagram is depicted in Fig. 7 (a), while (b) shows the corresponding plot of imaginary and real parts of the eigenvalues versus γ. The four exceptional points are easily obtained from $\frac{\partial G(s)}{\partial s} = 0$ resulting in $\pm\omega_0$ and $\pm i\,\omega_0$. These results agree with those presented in the literature [25]. As $n \to \infty$, the oscillator chain tends to behave like a transmission line.

7 Conclusions

The presented proposal allows a systematic approach to the analysis of an oscillator chain exhibiting non-Hermiticity. The inclusion of feedback as a mechanism for non-Hermiticity opens the door to the use of a vast amount of tools and techniques for the study and design of structures presenting $\mathcal{PT}$ symmetries, giving insight on the behavior of those systems. The approach allows an easy determination of the range of the parameters that ensure real-valued eigenvalues for non-Hermitic Hamiltonians and characterizes the spontaneous symmetry breaking occurring at exceptional points. Applications could include, among others, optics, photonics, and biological oligomers.

References

[1] C. M. Bender, "Making sense of non-Hermitian Hamiltonians", Rep. Prog. Phys. 70, 947 (2007) doi:10.1088/0034-4885/70/6/R03

[2] Y, Ashida, Z. Gong, M. Ueda, "Non-Hermitian physics", Advances in Physics, vol. 69 number 3, pp 249-435, Taylor & Francis 2020. DOI:10.1080/00018732.2021.18.76991

[3] J Schindler, Z Lin, J M Lee, H Ramezani, F M Ellis and T. Kottos, "PT -symmetric electronics". Journal of Physics A: Math. Theor. 45

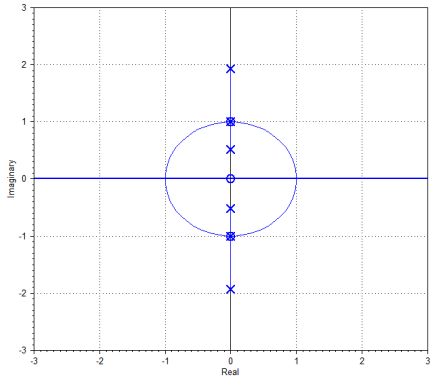

(a)

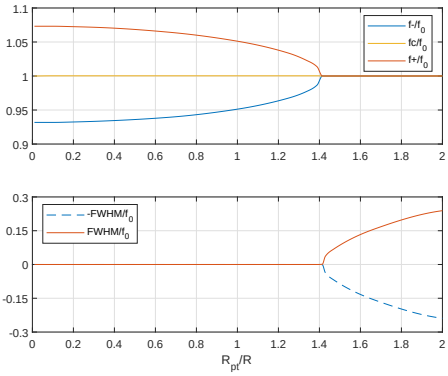

(b)

Figure 7: Simulation results for the trimer.(a) Root-locus. (b): Normalized imaginary an real parts vs. normalized degree of Hermiticity

[4] J. Schindler, Ang Li, Mei C. Zheng, F. M. Ellis, and T. Kottos, "Experimental study of active LRC circuits with PT symmetries". Phys. Rev. A 84, 040101(R) – 2011. DOI:10.1103/PhysRevA.84.040101 (2012). doi:10.1088/1751-8113/45/44/444029.

[5] Hamidreza Ramezani, J. Schindler, F. M. Ellis, Uwe Gunther, Tsampikos Kottos, "Bypassing the bandwidth theorem with PT symmetry". Physical Review A 85, 062122 (2012). DOI: 10.1103/PhysRevA.85.062122

[6] M. S akhdari , M. Hajizadegan , Q. Zhong , D. N. Christodoulides, R. El-Ganainy,2, P.-Y. Chen1, "Experimental Observation of PT Symmetry Breaking near Divergent Exceptional Points", Physical Review Letters 123, 193901 (2019). DOI:https://doi.org/10.1103/PhysRevLett.123.193901

[7] C, M. Bender, M. Gianfreda, S. P. Klevansky, "Systems of coupled PT -symmetric oscillators". Physical Review A 90, 022114 (2014)DOI: 10.1103/PhysRevA.90.022114

[8] W. Evans , "Graphical Analysis of Control Systems", Trans. AIEE, 67 (1)(1948): 547–551, doi:10.1109/ T-AIEE.1948.5059708.

[9] Kuo, B. C., "Automatic control systems", Prentice-Hall Englewood Cliffs, N.J 1975.

[10] Maryam Sakhdari et al, "PT-symmetric metasurfaces: wave manipulation and sensing using singular points". 2017 New J. Phys. 19 065002. DOI 10.1088/1367-2630/aa6bb9

[11] Mohamed Farhat, Minye Yang, Zhilu Ye, and Pai-Yen Chen, "PT-Symmetric Absorber-Laser Enables Electromagnetic Sensors with Unprecedented Sensitivity". ACS Photonics 2020 7 (8), 2080-2088. DOI: 10.1021/acsphotonics.0c00514

[12] M. Hajizadegan, M. Sakhdari, S. Liao and P. -Y. Chen, "High-Sensitivity Wireless Displacement Sensing Enabled by PT-Symmetric Telemetry," in IEEE Transactions on Antennas and Propagation, vol. 67, no. 5, pp. 3445-3449, May 2019, doi: 10.1109/TAP.2019.2905892.

[13] M. Caruso, H. Fanchiotti, C. A. García Canal, M. Mayosky and A. Veiga, "The quantum CP-violating kaon system reproduced in the electronic laboratory", Proceedings of the Royal Society A, (2016). Volume 472, Issue 2195. DOI:10.1098/rspa.2016.0615

[14] K. M. Adams, E. F. A. Deprettere and J. O. Voorman (1975). Ladislaus Marton (ed.). "The gyrator in electronic systems". Advances in Electronics and Electron Physics. Academic Press, Inc. 37: 79–180. doi:10.1016/s0065-2539(08)60537-5. ISBN 9780120145379.

[15] O.N. Kirillov, "PT-symmetry, indefinite damping and dissipation-induced instabilities". Physics Letters A, 376(15): 1244-1249. 2012. DOI:10.1016/j.physleta.2012.02.055

[16] O.N. Kirillov, "Stabilizing and destabilizing perturbations of PT -symmetric indefinitely damped systems". Philosophical Transactions of the Royal Society A, 371: 20120051. 2013. doi:10.1098/rsta.2012.0051

[17] H. Fanchiotti, C. A. Garcia Canal, M. Mayosky, A. Veiga, V. Vento, "Measuring the Hannay geometric phase", ArXiv: 2111. 13150 [physics. class-ph] https:// doi.org/ 10.48550/ arXiv.2111.13150

[18] W. Evans , "Control Systems Synthesis by Root-locus Method", Trans. AIEE, 69 (1) (1950): 66–69, doi: 10.1109/ T-AIEE. 1950.5060121.

[19] Skilling, H.H., "Electrical Engineering Circuits", McGraw-Hill electrical and electronic engineering series, Wiley 1965.

[20] C. Cortes, Z. Jacob,"Quantum maximum power transfer theorem", arXiv:1904.08866v1 [quant-ph] 18 Apr 2019.

[21] Q factor, https://en.wikipedia.org/w/index.php?title=Qfactor.

[22] M. Engelhardt, "LT-spice IV User Manual", Analog Devices, https:// www. analog. com/ en/ design-center/ design-tools-and-calculators/ ltspice-simulator. html. 2022.

[23] John R Silvester. "Determinants of Block Matrices". Mathematical Gazette, The Mathematical Association, 2000, 84 (501), pp.460-467. ff10.2307/3620776ff. ffhal-01509379f

[24] Wen-Chyuan Yueh, "Eigenvalues of several tridiagonal matrices". Applied Mathematics E-Notes, 5:66–74, 2005.

[25] C. Downing, V. Saroka, "Exceptional points in oligomer chains", Communication Physics (2021) 4:254. DOI: /10.1038 /s42005-021-00757

Appendix A Spontaneous symmetry breaking

As it is well known in Quantum Mechanics, an operator $\mathcal{PT}$ represents a symmetry if it commutes with the Hamiltonian of the system, namely

$$[H, \mathcal{PT}] = (H\,\mathcal{PT} - \mathcal{PT}\,H) = 0$$

As mentioned in the main text, the $\mathcal{PT}$-symmetry is spontaneously broken (triggered by parameter γ) when it goes through an exceptional point. In the symmetric phase, the Hamiltonian has real eigenvalues below the exceptional point $\gamma^\star$, and complex conjugate ones above it. Explicitly

$$H\,\psi_{1,2} = \lambda_{1,2}\,\psi_{1,2}$$

with λ_1 and λ_2 real for $\gamma < \gamma^\star$ and with complex $\lambda_2 = \lambda_1^\star$ for $\gamma > \gamma^\star$

As was stated before, the presence of the symmetry implies that

$$H\,(PT)\,\psi_{1,2} = (PT)\,H\,\psi_{1,2} = (PT)\,(\lambda_{1,2}\,\psi_{1,2})$$

and in the region where the eigenvalues are real one has

$$PT\,(\lambda_{1,2}\,\psi_{1,2}) = \lambda_{1,2}\,(PT\,\psi_{1,2})$$

meaning that $\mathcal{PT}\,\psi_{1,2}$ is also eigenfunction of H and that $\psi_{1,2}$, the solution, has the same symmetry that the one present in the Hamiltonian. In this region the symmetry is said to be Wigner-Weyl realized.

Above the exceptional point $\gamma^\star$ the situation is different because the symmetry operator also acts on the complex eigenvalues conjugating them,

$$H\,(\mathcal{PT})\,\psi_1 = (\mathcal{PT})\,(\lambda_1\,\psi_1) = \lambda_1^\star(\mathcal{PT})\,\psi_1 = \lambda_2\,(\mathcal{PT})\,\psi_1$$

or

$$(\mathcal{PT})\,\psi_1 = \psi_2$$

which explicitly shows that the $\mathcal{PT}$ symmetry is not present in the solution and turns one solution to the other. This is the natural appearance of the *spontaneous symmetry breaking*. The symmetry of H has a Nambu-Goldstone realization because the solutions do not respect it.